Ultrastructural anatomy of CALT follicles in the rabbit reveals characteristics of M-cells, germinal centres and high endothelial venules

Nadja Knop[1] and Erich Knop[2]

[1]*Department for Cell Biology in Anatomy, Hannover Medical School, Hannover, Germany*
[2]*Research Laboratory of the Eye Clinic CVK, Charite – University School of Medicine, Berlin, Germany*

Abstract

Conjunctiva-associated lymphoid tissue (CALT) is a part of the eye-associated lymphoid tissue (EALT) at the ocular surface. Its lymphoid follicles are usually characterized by using light microscopy, but its ultrastructure remains largely unknown. In this study, flat whole-mount conjunctival tissues (*n* = 42) from 21 young adult rabbits were investigated native in reflected light, and further stained and cleared (*n* = 6), in paraffin histology sections (*n* = 6), scanning electron microscopy (SEM, *n* = 4) and transmission electron microscopy (TEM, *n* = 4). Secondary lymphoid follicles accumulated into a dense group nasally towards the lacrimal punctum of the lower lid. High endothelial venules (HEV) with typical ultrastructure occurred in the parafollicular zone. The bright germinal centre (GC) contained lymphoblasts, follicular dendritic cells, apoptotic cells and tingible body macrophages. The follicle-associated epithelium (FAE) was devoid of goblet cells and contained groups of lymphoid cells. TEM showed these cells to be located in cytoplasmic pockets of superficial electron-lucent cells with a thin cytoplasmic luminal lining that contained a fine filament meshwork and numerous endocytotic vesicles. These M-cells were sitting between and on top of the ordinary dense epithelial cells that were located basally and formed pillar-like structures. In stereoscopic SEM, the surface cells were very large, had a polygonal outline and covered cavernous spaces. The rabbit has a CALT with typical follicular morphology, including HEV for regulated lymphocyte migration and epithelial cells with ultrastructural characteristics of M-cells that allow antigen transport as indicated by the GC-reaction. The arrangement of these M-cells on top of and between epithelial pillar cells may reflect a special structural requirement of the multilayered CALT FAE.

Key words conjunctiva-associated lymphoid tissue (CALT), eye-associated lymphoid tissue (EALT), high endothelial venules (HEV), lymphoid follicles, M-cells, mucosal immunity.

Introduction

The mucosa-associated lymphoid tissue (MALT) represents a part of the immune system of the body that is located in organs with mucosal surfaces. These surfaces are connected by lymphocyte recirculation and form the common mucosal immune system (Bienenstock et al. 1978; Mestecky et al. 1978) in order to provide immune protection (Brandtzaeg, 1996; McGhee et al. 1999). Lymphoid tissue also occurs at the ocular surface and had been described in the rabbit in the nineteenth (Virchow, 1910) and early twentieth (Niimi, 1935) centuries. Later, its renewed description in this species led to the introduction of the term 'conjunctiva-associated lymphoid tissue' which was abbreviated to CALT (Axelrod & Chandler, 1979) according to the then-existing nomenclature for MALT tissue in the body. Its continuation into the rabbit lacrimal drainage system was also reported (Knop & Knop, 1996). CALT has also been described in several other animal species (Chodosh et al. 1998b; Chodosh & Kennedy, 2002).

The most obvious components of MALT are lymphoid follicles that serve as the afferent limb of the immune system. Here lymphocytes come into contact with antigens from the luminal surface and undergo proliferation and differentiation in the germinal centre (GC) reaction to mature into effector cells of the cellular immune response (T-cells) or into immunoglobulin-secreting plasma cells. Lymphocytes enter lymphoid tissues coming from the bloodstream mainly via specialized high endothelial venules (HEV) (Gowans & Knight, 1964; Kraal & Mebius, 1997). They leave the tissue via lymphatic vessels and can eventually return via the thoracic duct into the blood circulation (Pabst & Westermann, 1997). In this way the arising effector cells can populate the same or other organs of the mucosal immune system as a result of recirculation of lymphoid cells in the body (Butcher & Picker, 1996; Knop & Knop, 2004b).

Antigen transport through the follicle-associated epithelium (FAE) is physiologically maintained by a special population of cells (Neutra et al. 1996b; Gebert, 1997). These cells are also relevant as gateways for mucosal microbial infection (Wolf et al. 1981) and as potential targets for therapeutic immunization and drug delivery (Neutra et al. 1996a; Jepson et al. 2004). Their surface is exposed to the mucosal lumen and they form a cytoplasmic pocket that contains mainly lymphoid cells that are separated from the lumen only by a thin layer of cytoplasm. The term 'M'-cells was chosen for them because in the small intestine, from which they were first described, they have a surface that is different from the surrounding epithelial cells with numerous microvilli and are characterized as 'membranous' (smooth) or 'microfolded' (Owen & Jones, 1974). In fact, M-cells represent a cell type with fairly inhomogeneous morphology even in the different parts along the intestine (Jepson et al. 1993; Gebert et al. 1996).

Conjunctival M-cells were first described in the guinea-pig (Latkovic, 1989) and later also in other species, e.g. monkey (Ruskell, 1995; Ruskell & VanderWerf, 1997), rabbit (Knop & Knop, 1998c,d) and in the nictitating membrane of the dog (Giuliano et al. 2002). In the rabbit the follicles were mainly described from histology sections (Axelrod & Chandler, 1979; Franklin & Remus, 1984; Chodosh et al. 1998b) with additional scanning electron microscopy (SEM) findings of cells with longer microvilli in this area (Chandler & Axelrod, 1980). We have described ultrastructural SEM and transmission electron microscopy (TEM) characteristics of CALT in the rabbit (Knop & Knop, 1996), including apical follicle-associated epithelial cells with morphological characteristics of M-cells (Knop & Knop, 1998c,d). Selective uptake of substances was described over rabbit CALT follicles for polystyrene microparticles (Liu et al. 2004) and for iron oxide in a paper that appeared during submission of the present manuscript (Astley & Chodosh, 2005).

CALT is a part of the eye-associated lymphoid tissue (EALT) (Knop & Knop, 2002) that unites the human ocular surface and appendage from the lacrimal gland-associated lymphoid tissue (Knop & Knop, 2003) over the conjunctiva (Knop & Knop, 2000) into the lacrimal drainage-associated lymphoid tissue (LDALT) (Knop & Knop, 2001; Paulsen et al. 2002). EALT has important implications for the preservation of physiological immunological homeostasis and for the local generation of effector cells against antigens that occur at the ocular surface (Knop & Knop, 2005). In cases of deregulation, however, EALT can also be involved in the course of inflammatory processes at the ocular surface (Knop & Knop, 2002, 2004a; Stern et al. 2002) that are increasingly recognized to contribute to a number of diseases, such as dry eye syndrome, ocular allergy and corneal transplant rejection (Dana et al. 2000; Pflugfelder et al. 2000; Knop et al. 2003, 2004).

There has thus been renewed interest in the ocular mucosal immune system and in M-cells as important mediators of the afferent immune function. We re-investigated these structures in the rabbit conjunctiva by using light microscopy together with SEM and TEM. We focused on the ultrastructure of the CALT follicle FAE with M-cells, on the GC and on the parafollicular HEV.

Materials and methods

Complete conjunctival sacs from normal young adult New Zealand White rabbits ($n = 12$) and Chinchilla rabbits ($n = 9$) were obtained according to the Association for Research in Vision and Opthalmology (ARVO, www.arvo.org) guidelines for animal research. Tissue preparation started from the lid margin, which was preserved together with the eyelashes. We separated the posterior lid lamella including the conjunctiva and proceeded over the fornix to the limbus, as previously described for the human (Knop & Knop, 2000). The complete conjunctival sac including the nictitating membrane was thus obtained and prepared as a flat whole-mount on a silicone mat. These specimens were investigated by different techniques:

1 All native 42 conjunctival whole-mount specimens were viewed in reflected light with a stereo magnifier (Wild-Leitz, Leica, Bensheim, Germany) for analysis of the presence and distribution of lymphoid follicles; no difference was observed between the two strains.

2 Six conjunctival sacs from these specimens were fixed by immersion in 4% paraformaldehyde, freshly prepared from powder (Sigma, München, Germany) in 0.01 M phosphate buffer, at 4 °C overnight and washed in the same buffer. The tissues were later stained with undiluted Mayer's haematoxylin (Merck, Darmstadt, Germany) for 10 min, cleared by immersion in an anise oil mixture as applied by Kessing (1968) and originally described by Aurell (1938). The tissues were then mounted in this medium between object glass slides and observed in transmitted light with a stereo magnifier.

3 Six conjunctival sacs were fixed at 4 °C overnight by immersion in the described 4% paraformaldehyde solution and washed in 0.01 M phosphate buffer. They were dehydrated in a graded ethanol series and embedded via 2-propanol intermedium into paraffin (Histocomp, Vogel, Giessen, Germany). Paraffin sections 5 μm thick were obtained with a rotating microtome (Reichert, Leica), stained with haematoxylin–eosin and investigated and photo documented by light microscopy (Dialux 22, Leica).

4 Four conjunctival sacs were fixed by immersion in a mixture of 2.5% glutaraldehyde and 2% para-formaldehyde in 0.1 M cacodylate buffer (according to Karnovsky, 1965) and later washed in the same buffer. Regions of interest were then cut out, postfixed in osmium tetroxide dehydrated in a graded ethanol series, embedded via toluene intermedium into epoxy resin (Agar 100, Serva, Heidelberg, Germany) and sections were cut with a rotating microtome (Reichert Ultracut, Leica). Semithin 1-μm sections stained with toluidine blue were investigated by light microscopy. Thin sections (70 nm) were prepared for TEM as previously described (Knop & Knop, 2000), obtained on copper grids, stained with lead citrate and uranyl acetate, and investigated in a EM10 (Zeiss, Göttingen, Germany).

5 For investigation of the surface ultrastructure, four flat mounted conjunctival sacs were fixed by immersion in the same aldehyde mixture (Karnovsky, 1965). Complete conjunctival sacs were further treated for SEM by dehydration in a graded acetone series, by drying according to the critical-point method with CO_2 (Smith & Finke, 1972) in a Balzers CPD 020 (Baltec, Schalksmühle, Germany) and by additional sputter coating with gold–palladium (Balzers SCD, Baltec). Specimens were investigated in a SEM 505 (Philips, Eindhoven, The Netherlands) scanning electron microscope with an object stage that can be tilted in order to allow stereoscopic SEM images.

Results

Follicle distribution

Lymphoid follicles were detectable as light reflections during macroscopic inspection of unstained native conjunctival tissues and appeared as prominent clear elevations of the surface under the stereo magnifier. The follicles appeared to be co-localized with the course of larger stromal blood vessels (Fig. 1A). In conjunctival whole-mounts stained with haematoxylin and later optically cleared, follicles were detectable as roundish dark spots of different size (not shown). Close examination showed that in the lower lid they typically accumulated nasally towards the area where the only lacrimal punctum is located close to the base of the nictitating membrane and the caruncle. This follicle zone was more clearly detectable in low-magnification views of specimens prepared for SEM (Fig. 1B). Towards the lacrimal punctum, the follicles increased in size and were densely aggregated resembling Peyer's patches in the intestine. Towards the other zones of the lower lid solitary follicles decreased in size and were increasingly separated and distributed over a wider area (Fig. 1B).

Characteristics of rabbit CALT follicles

Histological paraffin sections of conjunctival whole-mounts revealed accumulations of follicles in the described nasal position (Fig. 2A). Most had a bright germinal centre encircled at the top and lateral sides by a dense corona of lymphocytes. Light microscopical analysis of semithin sections from resin-embedded tissues (Fig. 2B–F) showed that the epithelium overlying the apex had clear characteristics of FAE (Fig. 2D,E). Goblet cells terminated at the follicular flanks and were absent from the FAE, which regularly contained numerous lymphocytes, frequently arranged in groups (Fig. 2B–D). In cross and tangential sections (Fig. 2B,C) cells with a relatively dark cytoplasm were detected in the FAE. In cross sections (Fig. 2B) they consisted of basal cells, which piled up or assumed an elongated shape and formed pillar-like structures that separated the lymphoid cells. In tangential sections (Fig. 2C) they formed roundish
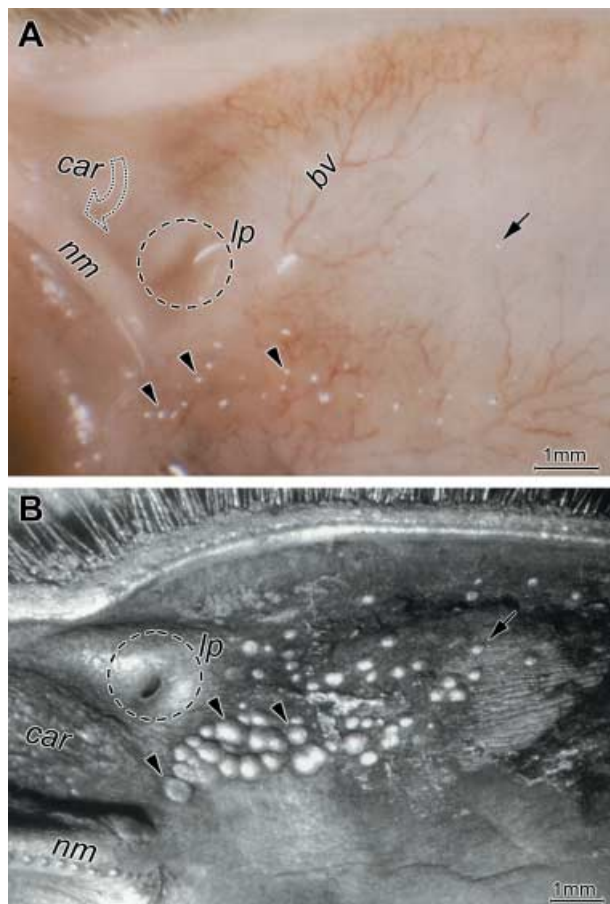
Fig. 1 Lymphoid follicles at the surface of the rabbit conjunctiva (here in the lower lid) are seen as light reflections (A) in a native whole-mount tissue with a stereo magnifier and as prominent roundish structures, also with white reflections, in a specimen prepared for SEM (B). Follicles are aggregated in a group (arrowheads) nasally in the area where the base of the nictitating membrane (nm) meets the lacrimal punctum (lp, encircled) and the caruncle (car). Solitary follicles (arrows) are distributed as over the rest of the conjunctival surface. The nictitating membrane is tilted downwards in the native tissue and partly hides the caruncle (open arrow in A). The follicles appear co-localized with blood vessels (bv in A); scale bars = 1 mm.

fence-like structures that encircled the lymphoid cells among which single, large, pale nuclei were seen. Numerous vessels occurred in the parafollicular zone (Fig. 2E,F). Prominent lymph vessels were always present together with numerous HEV. Arterioles, as seen in the native tissues (Fig. 1A), were located at the border to and deeper within the conjunctival stroma (Figs 2E and 3A).

Parafollicular vessels including HEV

In the parafollicular zone beneath the follicles, distinct, occasionally large, lymphatic vessels with lymphocytes in the lumen were regularly found lying in a lymphoid tissue. Numerous lymphoid cells, fibroblastic reticulum cells with large bright roundish nucleus and large cytoplasm as well as macrophages with an irregularly shaped or indented nucleus were embedded in a loose connective tissue with distinct bundles of collagen fibrils. Sometimes lymphocytes where seen directly adjacent to the vessels and formed groups beneath the basement membrane or aligned as if they were guided to the vessel. Arterioles were characterized by 2–3 layers of smooth muscle cells in the wall and encircled by a collageneous adventitia (Fig. 3A).

HEV were numerous in the parafollicular zone and also extended into the underlying dense stroma (Fig. 3B). The typical HEV morphology with bright cuboidal endothelial cells continued until they left the parafollicular zone. At the transition to the dense collageneous stroma the endothelial cells gradually became flat and the vessels transformed into ordinary post-capillary venules; this transformation could be studied if an HEV was viewed in tangential section (Figs 2E and 3B). Lymphocytes were seen inside the lumen of the HEV in all stages of emigration and also as groups in the vicinity of the vessels.

In TEM (Fig. 4A–D), it could be observed that the HEV were connected by numerous lateral interdigitations (Fig. 4A,C). These cells had few intercellular junctions, which were seen as dark dots or longer extensions, contained dense material in the intercellular cleft but lacked a distinct dark attachment plaque as characteristic for desmosomes and hence represented zonulae adherentes (Fig. 4B,C). They had numerous filopodia at their basal surface towards the basement membrane and their apical surface formed lamellopodia if it was in contact with lymphocytes. The endothelial cells contained free ribosomes, single cisternae of rough endoplasmic reticulum, mitochondria and a distinct Golgi apparatus which was located at the apical cell pole towards the lumen (Fig. 4C,D). Vesicles originating from the Golgi filled the apical cytoplasm and fused with the cell membrane.

The HEV wall consisted, in addition to endothelial cells and their basement membrane, of several adjacent, narrow, concentric sheets of the cytoplasm of pericytes that were covered by their own basement membrane. They contained few organelles but frequent microfilaments and dense attachment bodies beneath the cell membrane and inside the cytoplasm (Fig. 4A,B), indicating their contractile function.
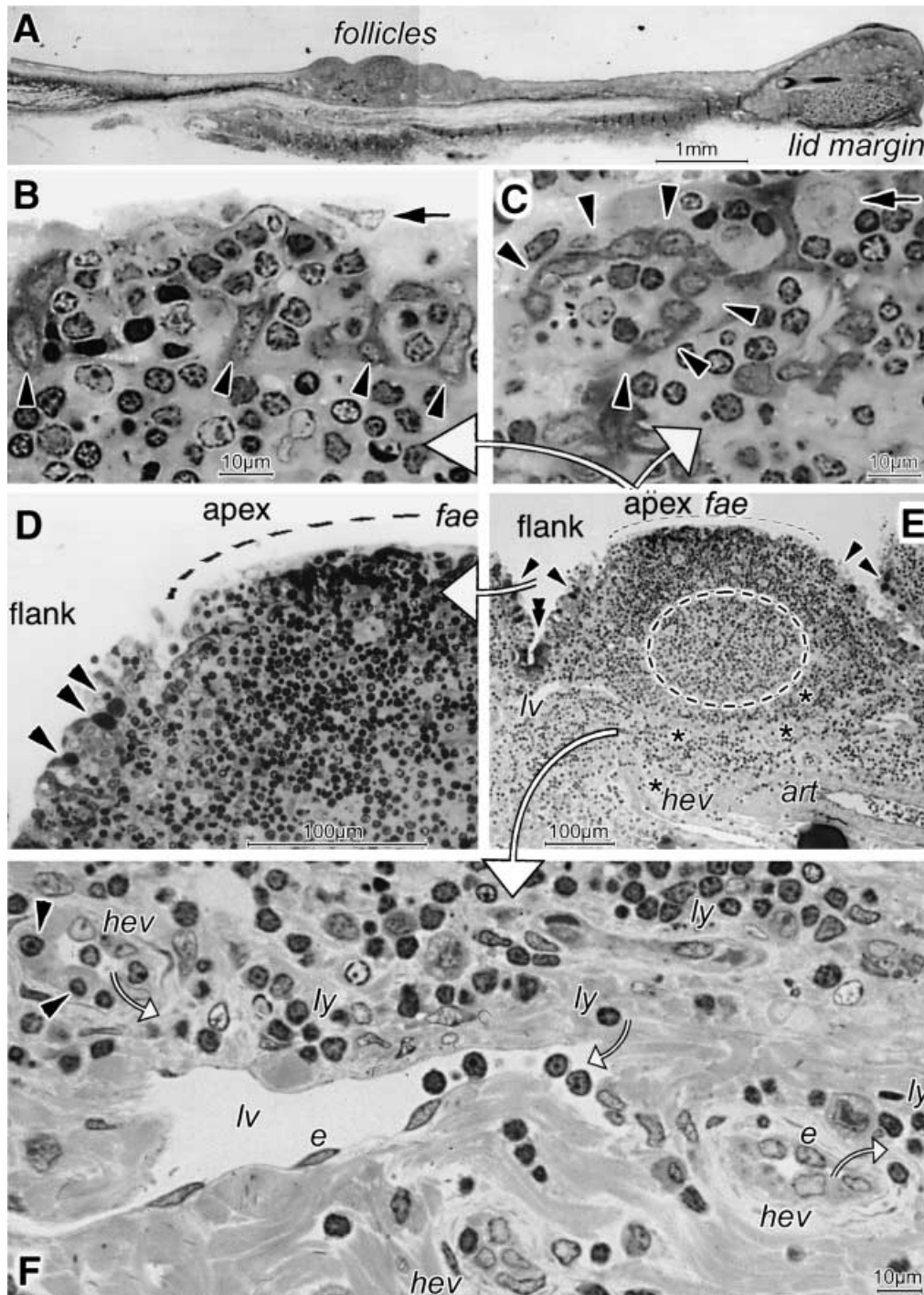
Fig. 2 A paraffin-embedded section reveals a nasal group of lymphoid follicles (A). These have typical characteristics, as seen in greater detail in semithin sections (B–E; large white arrows point from the follicle overview in E to enlarged details shown in panels B–D and F). The brighter germinal centre (interupted line in E) is encircled by a dense lymphocyte corona. Along the follicle flank the epithelium transforms into a specialized flat lined follicle-associated epithelium (fae) without goblet cells (arrowheads in D,E) at the apex. Crypts (E, double arrowhead) with dark cells occur between follicles. In the FAE, groups of lymphoid cells are separated by darker epithelial cells (arrowheads in B,C) that are arranged as pillars in cross section (B) and as fence-like structures in tangential section (C). On top of (B) and among (C) the lymphoid cells are large pale nuclei (arrows in B,C). In the parafollicular zone (E,F) are high endothelial venules (asterisks and hev) with bright roundish endothelial cells (e in F) and lymphoid cells in the lumen, inside their wall (arrowheads in F) and around (ly). Lymph vessels (lv), lined by ordinary flat endothelial cells (e), also contain lymphocytes. An arteriole (art in E) is at the border with the stroma. Small open arrows (F) indicate the presumed direction of lymphocyte migration, as known from the literature; scale bars = 1 mm in A, 100 μm in D,E, 10 μm in B,C,F.
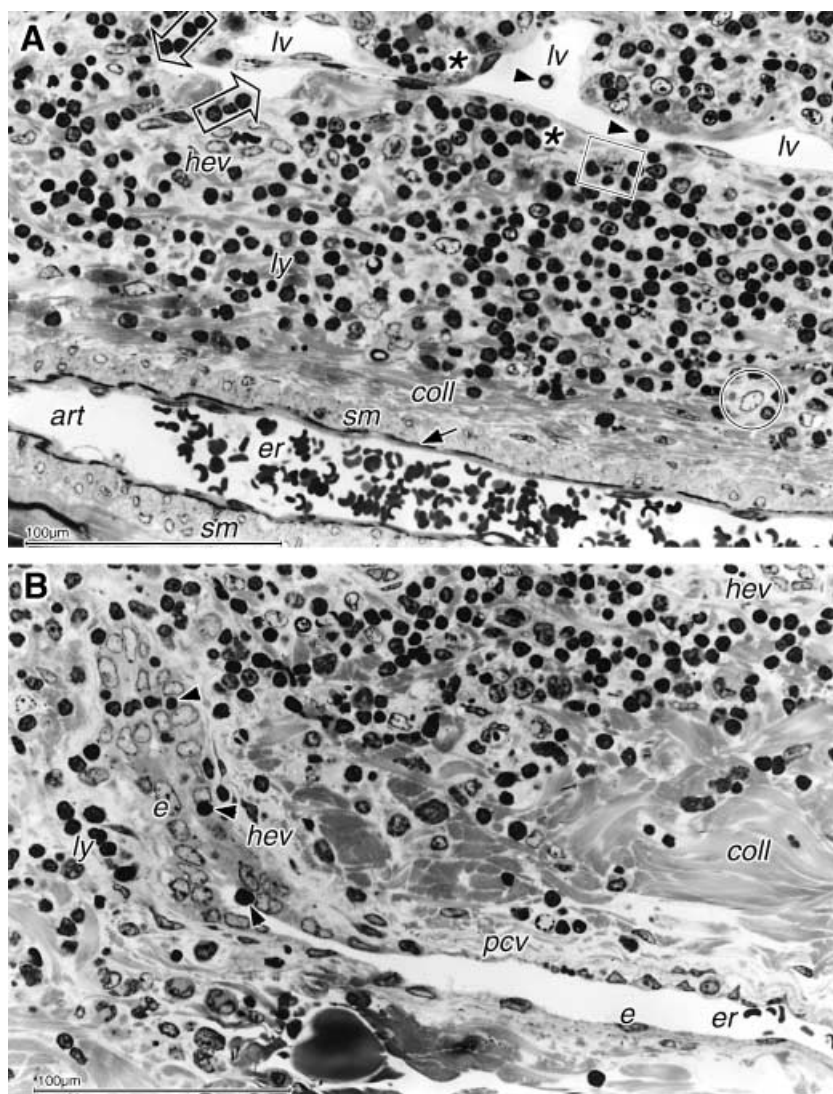
Fig. 3 Light micrographs of semithin sections showing details of vessels from Fig. 2(E). (A) The lymph vessel (lv) with lymphocytes in the lumen (arrowheads) occurs together with an arteriole (art), characterized by 2–3 layers of smooth muscle (sm) cells, an internal elastic membrane (arrow) and a collageneous adventitia (coll). Numerous lymphoid cells form a lymphoid tissue with interspersed reticulum cells (encircled) and macrophages (square); an HEV is also seen (hev). Lymphocytes occur in groups (asterisks) or align (open arrows) beneath the lymphatic endothelium. (B) The HEV (hev) from Fig. 2(E), viewed tangentially, extends from the parafollicular zone downwards. At the transition to the stroma where collagen fibril bundles (coll) become dense it changes its endothelial morphology from cuboidal into the flat shape of an ordinary post-capillary venule (pcv); erythrocytes (er) are present in the lumen. One lymphocyte (arrowhead) in the HEV lumen adheres to the endothelial cells, and others are seen during transmigration (arrowheads) between the cuboidal cells (e) and also in the vicinity (ly). Scale bars = 100 μm.

Germinal centre

The bright GC of the lymphoid follicles was occupied by densely packed cells, including different cell types with large cytoplasm, and hence appeared less electron dense than the rest of the follicle (Fig. 5A,B). Only few collagen fibrils occurred in this area. Lymphoblasts with a larger cytoplasm than that of the usual small, resting lymphocytes, contained more organelles, including several mitochondria, and had an more euchromatic nucleus which could still be round or assumed an irregular shape. Apoptotic lymphocytes with a small dark nucleus filled by peripheral dark masses of heterochromatin were interspersed. Large follicular dendritic cells (FDC), which had a highly euchromatic nucleus of roundish or oval shape and occasional large nucleoli, sent long cytoplasmic processes between the lymphoid

cells. The cytoplasm of these cells contained the usual organelles together with frequent vesicles generally < 1 μm in diameter. This cytoplasmic composition also extended into their processes, together with microfilaments and bundles of microtubules (Fig. 5B). Tingible body macrophages were detected by an irregularly shaped or indented nucleus and numerous lysosomes and phagolysosomes in the cytoplasm, which presumably contained the remnants of internalized apoptotic lymphocytes.

Interfollicular secretory crypts

Infoldings of the surface epithelium formed crypts between the follicles that were lined by dark epithelial cells (Fig. 2E). At high magnification they were shown to consist of columnar cells with frequent apical dark
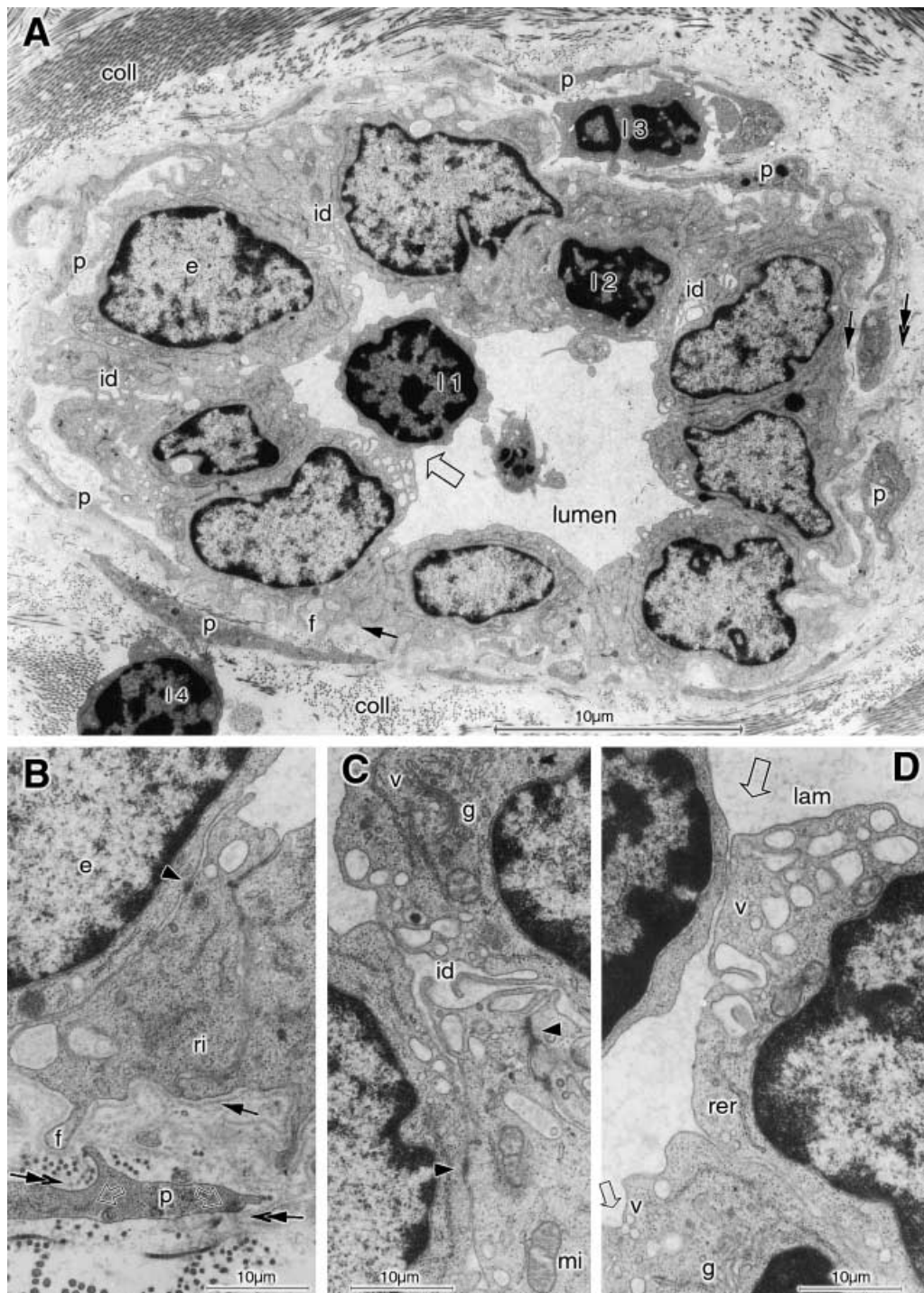
Fig. 4 TEM of an HEV in cross section, located among bundles of collagen (coll) fibrils, shows details in overview (A) and at high magnification (B–D). The cuboidal endothelial cells (e) have a euchromatic nucleus, lateral interdigitations (id in A,C), basal filopodia (f in A,B) and few intercellular junctions (arrowheads in B,C). In the cytoplasm are ribosomes (ri in B), cisternae of rough endoplasmic reticulum (rer in D) and mitochondria (mi in C). Small vesicles (v in C,D) from the apical Golgi apparatus (g in C,D) fuse with the plasma membrane (small open arrow in D) that forms lamellopodia (lam) where intraluminal lymphocytes are in contact with it (large open arrow in A,D). Narrow concentric layers of pericyte (p in A,B) cytoplasm, containing microfilaments and dense spots (open arrows in B), are ensheathed by their own basement membrane (double arrows in A,B) and form a part of the vessel wall. One lymphocyte (l1) in the lumen has made contact with an endothelial cell (open arrow in A,D); others are seen during transmigration among the endothelial cells (l2), between the pericyte lamellae (l3) and outside (l4) in contact with a pericyte. Scale bars = 10 μm in A, 1 μm in B–D.
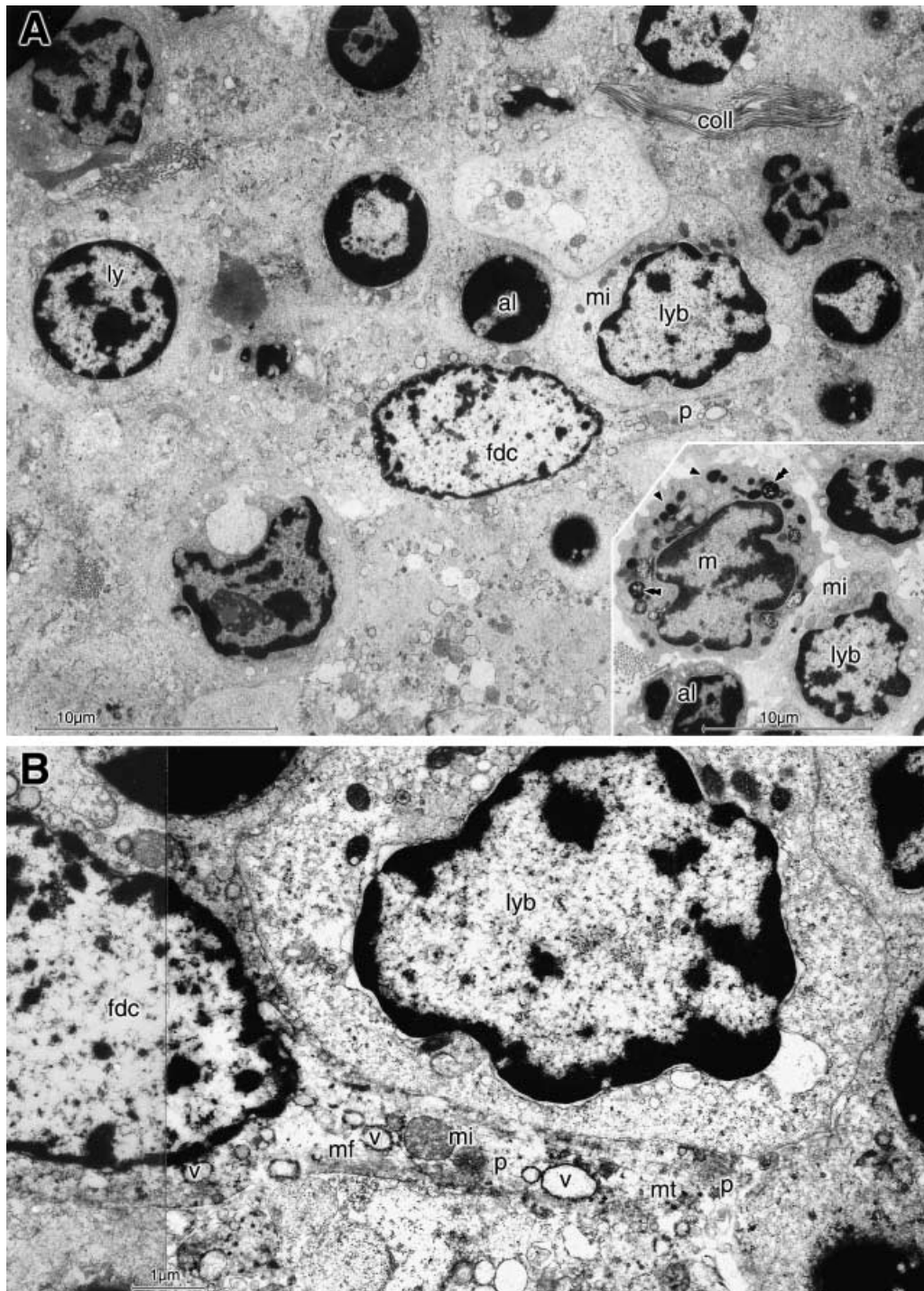
Fig. 5 The germinal centre is occupied by densely packed large cells (A) with only few collagen fibrils (coll). A large follicular dendritic cell (fdc), containing several medium-sized vesicles, extends a long cytoplasmic process (p) between the lymphoid cells. It is located among slightly enlarged lymphocytes (ly) with round nucleus, apoptotic lymphocytes (al) with a small dark nucleus and a lymphoblast (lyb) with irregularly shaped euchromatic nucleus and several mitochondria (mi); another potential lymphoblast is adjacent. Nearby (inset in A) is a tingible body macrophage (m) that has an indented nucleus and contains numerous lysosomes (arrowheads) and phagolysosomes (double arrowheads). It is surrounded by an apoptotic lymphocyte (al) and a lymphoblast (lyb) with mitochondria (mi). In B, the process (p) of the FDC, closely adjacent to the lymphoblast, is seen to contain microfilaments (mf), mitochondria (mi), microtubules (mt) and multiple vesicles (v). Scale bars = 10 μm in A and inset, 1 μm in B.
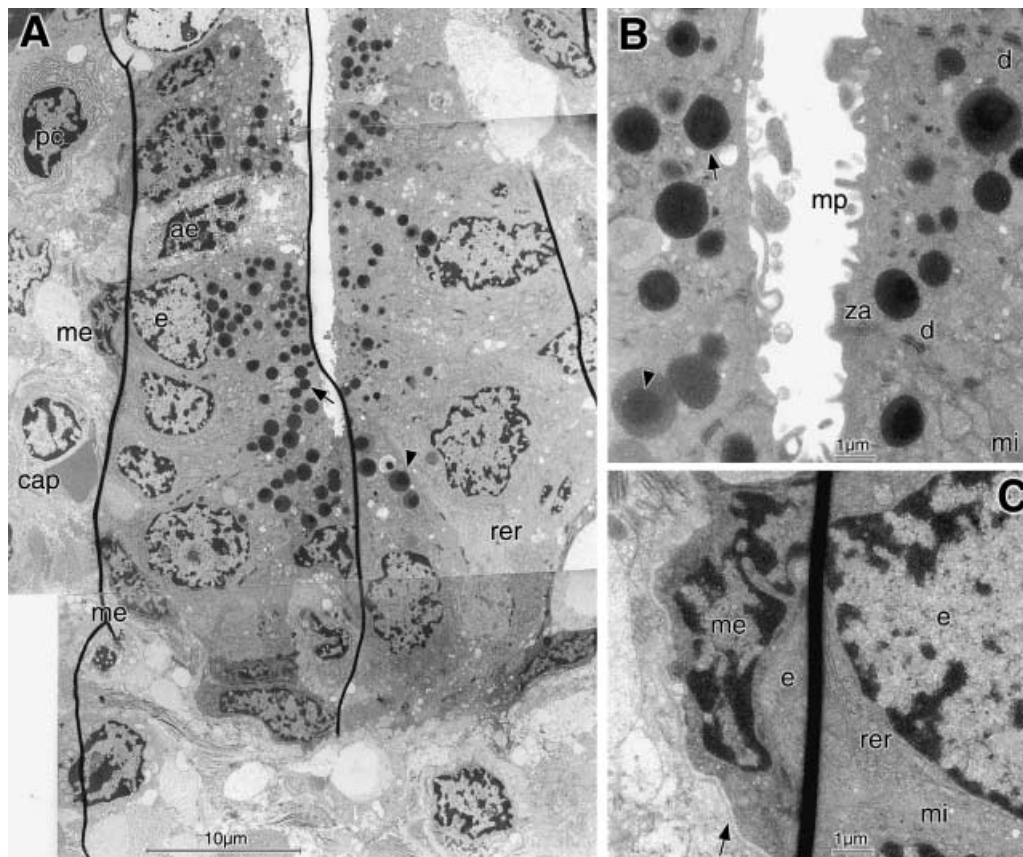
Fig. 6 Crypts (A–C) with secretory epithelial cells are located between the lymphoid follicles. The epithelial cells (e) have euchromatic nuclei and numerous apical secretory granules of different size. The dark core, obvious in immature brighter granules (arrowheads in A,B), is less obvious in mature dark granules (arrows). Frequent rough endoplasmic reticulum (rer in A,C) and mitochondria (mi in B,C) are present. Narrow myoepithelial cells (me in A,C) with constricted nuclei (see in C) surround the secretory cells and are enclosed together with them by a common basement membrane (arrow in C). The secretory cells have frequent lateral desmosomes (d in B), zonulae adherentes (za in B), and some luminal microprojections (mp in B); one cell is apoptotic (ae in A). Adjacent to the crypt is a plasma cell (pc) and a capillary (cap). As an artefact the section contains some microfolds (dark lines in A,C). Scale bars = 10 μm in A and 1 μm in B,C.

secretory granules (Fig. 6A,B). The crypts had a narrow lumen just a few micrometres in width. The secretory epithelial cells had basal roundish euchromatic nuclei and contained many organelles, namely numerous mito-chondria, stacks of rough endoplasmic reticulum and a prominent Golgi apparatus (Fig. 6B,C). The apical membrane had short microprojections. The cells were connected by frequent desmosomes and zonulae adherentes at the lateral surface. The secretory granules were formed in the supra-nuclear area and decreased in size towards the apical membrane. They contained a dense central core that was obvious in the early, large, bright granules (of about 1.5 μm diameter) but was increasingly obscured when the granules became denser and smaller during maturation (Fig. 6B). Closely adjacent to the basal surface of the crypt epithelium were several flat myo-epithelial cells with constricted nuclei that

enclosed the secretory cells and were covered together with them by the same basement membrane (Fig. 6C).

Surface morphology of follicles and structure of FAE including M-cells

Stereoscopic SEM images of the lymphoid follicles showed them as very prominent and, in the nasal region, closely aggregated hemispheres (Fig. 7A,B). They had a roundish to oval shape and a size ranging from about 0.2 to 0.8 mm in the longest axis. Within this size range, the aggregated follicles in the nasal zone were typically larger than the solitary follicles distributed over the rest of the conjunctival surface; aggregated follicles could be almost confluent. At the follicular flanks the epithelium showed a rough and uneven surface, whereas the FAE at the apex was relatively smooth (Fig. 7A,B).
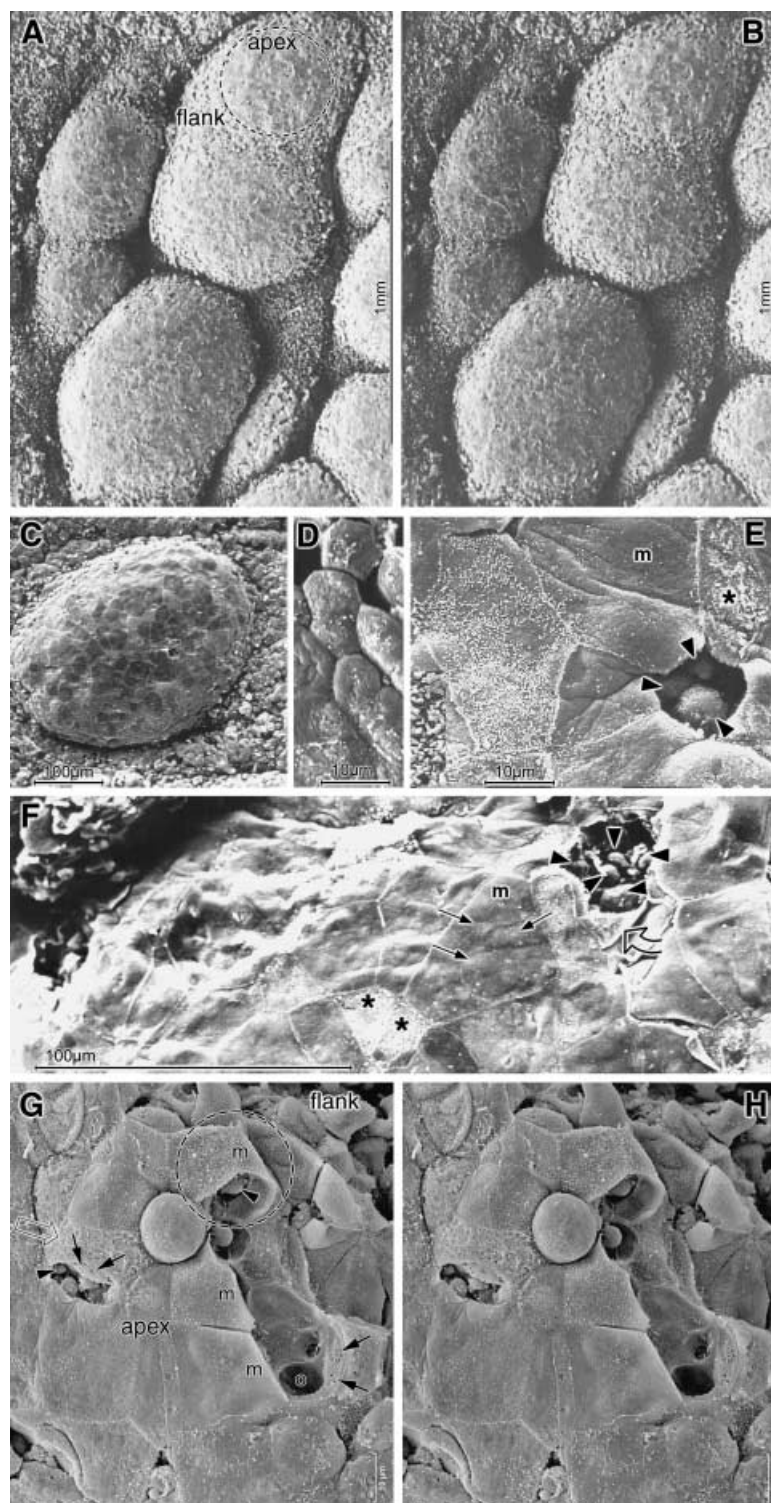
Fig. 7 SEM images of follicles show aggregated prominent round to oval hemispheres that are separated by deep clefts in stereoscopic figures (A,B) of the nasal region. A solitary follicle (C) is seen in conventional SEM. Cells at the apex (dashed circle in A) are flat, appear smooth and form a patchwork of cells with different brightness (C). In contrast to the surrounding small hexagonal epithelial cells (D), the FAE is composed of much larger cells (E). A large polygonal cell with smooth membranous surface (m in E) appears dark while the smaller one next to it has short inhomogeneously distributed microvilli and hence appears brighter. Cells where the membrane is destroyed also appear bright (asterisks in E,F). Where several cells meet, a small, probably natural, luminal opening occurs (E). Another cell is artificially fractured and the rest of its plasma is seen at the cell border (F, open arrow). Roundish cells are exposed beneath (arrowheads in E,F) or bulge the intact surface of a huge membranous cell (F, arrows). An apparently naturally shed cell leaves the surface of an underlying one intact but rough (G, open arrow). If membranous cells (m) are artificially fractured away, stereo images (G,H) show that they have a thin shell-like cytoplasm and cover deep cavernous spaces with smooth walls containing roundish cells (arrowheads). The walls have large basal openings (o) and smaller lateral ones arranged like sieve plates (arrow). The area marked by an interrupted circle (in G) resembles that seen in Fig. 8(A). Scale bars = 1 mm in A,B; 100 μm in C,F; 10 μm in D,E,G,H.

The FAE consisted of cells that were distinctly larger than the surrounding conjunctival epithelial cells (Fig. 7C–F). The latter were small hexagonal cells with a maximum surface diameter of 10 μm. The FAE, by contrast, was composed of a patchwork of large cells of variable brightness when viewed by SEM that had a polygonal shape and a diameter of 40–50 μm or more. Most of these cells, usually the larger ones, had a smooth

membranous surface with very few short microvilli which were mainly located along the cell borders. Other surface cells were somewhat smaller, had more frequent microvilli and hence appeared brighter when viewed by SEM (Fig. 7E), but the microvilli were often not evenly distributed and could leave membranous spots free. In places the superficial cell membrane appeared artificially destroyed or removed, completely or in part, indicating that these cells were very fragile (Fig. 7E–H).

There were occasional small luminal openings at locations where the borders of several cells met, and roundish cells were detectable beneath. Where superficial cells were completely detached, conceivably because of mechanical forces during the preparation process, groups of small roundish cells occurred beneath and the remaining detached plasma membrane was present at the cell border. In intact membranous cells, the surface was frequently bulged outward by underlying small roundish structures conceivably representing the cells seen exposed when the surface was detached (Fig. 7F). In some places SEM showed that the fractured superficial cells consisted of a thin delicate cytoplasm that formed a shell-like layer, beneath which were large hollow and interconnected spaces. The depth of these spaces can be judged on stereo images (Fig. 7G,H). At the basal side the spaces had large openings of about the size of lymphoid cells (5–10 μm) or larger. In the lateral wall other smaller openings of about 1 μm diameter occurred that were frequently arranged in a sieve plate fashion.

TEM of thin sections from the same areas revealed a similar architecture with an FAE permeated by groups of lymphoid cells (Fig. 8A). The FAE was built up by several layers of cells with electron-dense cytoplasm that rested on the basement membrane as basal cells and piled up or elongated to form longish upright pillars (Fig. 8A; compare with Fig. 2B). They had typical epithelial characteristics as dense cytoplasmic bundles of intermediate filaments. Between and on top of these cells were other cells with a narrow electron-lucent cytoplasm and a large euchromatic nucleus with occasional prominent nucleoli. Cells with an intermediate electron density were interposed between the dense and the lucent cells (Figs 8A,B and 9A). Higher magnification (Fig. 8B) revealed that the interposed cells lacked intermediate filament bundles or had only small and faint bundles and instead contained a meshwork of fine filaments. They had luminal vesicles similar to the electron-lucent cells but had some short microvilli in addition that were usually missing in the lucent cells. They may hence represent intermediate stages between the dense and the lucent cells and all three cell types were connected by frequent desmosomes.

The arrangement of the electron-dense epithelial cells formed cavities and these cells appeared as a mechanically supportive scaffold for the interposed lucent cells (Figs 8B and 9A). The cytoplasm of the electron-lucent cells formed a narrow (about 1–2 μm thick) cell plate at the luminal surface that was relatively smooth and usually contained no microvilli. Downwards, their cytoplasm also formed a narrow layer that lined the surrounding electron-dense cells like a thin wallpaper and enclosed the groups of lymphocytes in a cytoplasmic pocket, hence resembling epithelial M-cells (Fig. 9A). Occasionally lymphoid cells in the pocket appeared apoptotic. The wallpaper-like lining showed large openings at the basal sides corresponding in size to those observed in SEM, and also had much smaller lateral interruptions corresponding in size to the sieve plates seen in SEM (Fig. 7G,H). Often more than one M-cell spanned and formed a roof over the width of a basal cell cavity, and their cytoplasmic leaflets formed lateral septations that divided the epithelial cavity and overlapped at the luminal side for several micrometres (Fig. 9A); this is indicated in the schematic drawings in Fig. 10(A,B). The M-cell luminal cytoplasm contained numerous vesicles of about 100 nm diameter, including coated vesicles for receptor-mediated endocytosis (Fig. 9B); mitochondria, free ribosomes and few cisternae of the rough endoplasmic reticulum were also present. At the luminal surface, all stages of endocytotic vesicle formation were observed (Fig. 9B).

Discussion

The conjunctiva of the rabbit contains a CALT with secondary lymphoid follicles, as reported in previous studies (Axelrod & Chandler, 1979; Franklin & Remus, 1984; Knop & Knop, 1996; Chodosh et al. 1998b). The accumulation of lymphoid follicles into a dense zone nasally towards the lacrimal punctum as observed in all animals of the present study appears to be an undescribed phenomenon. This topography of CALT follicles that serve for antigen detection conceivably reflects the distribution and concentration of antigens at the ocular surface, as also found for CALT in the human (Knop & Knop, 2000), because it can be assumed that antigens in the tear film, after being washed off the ocular
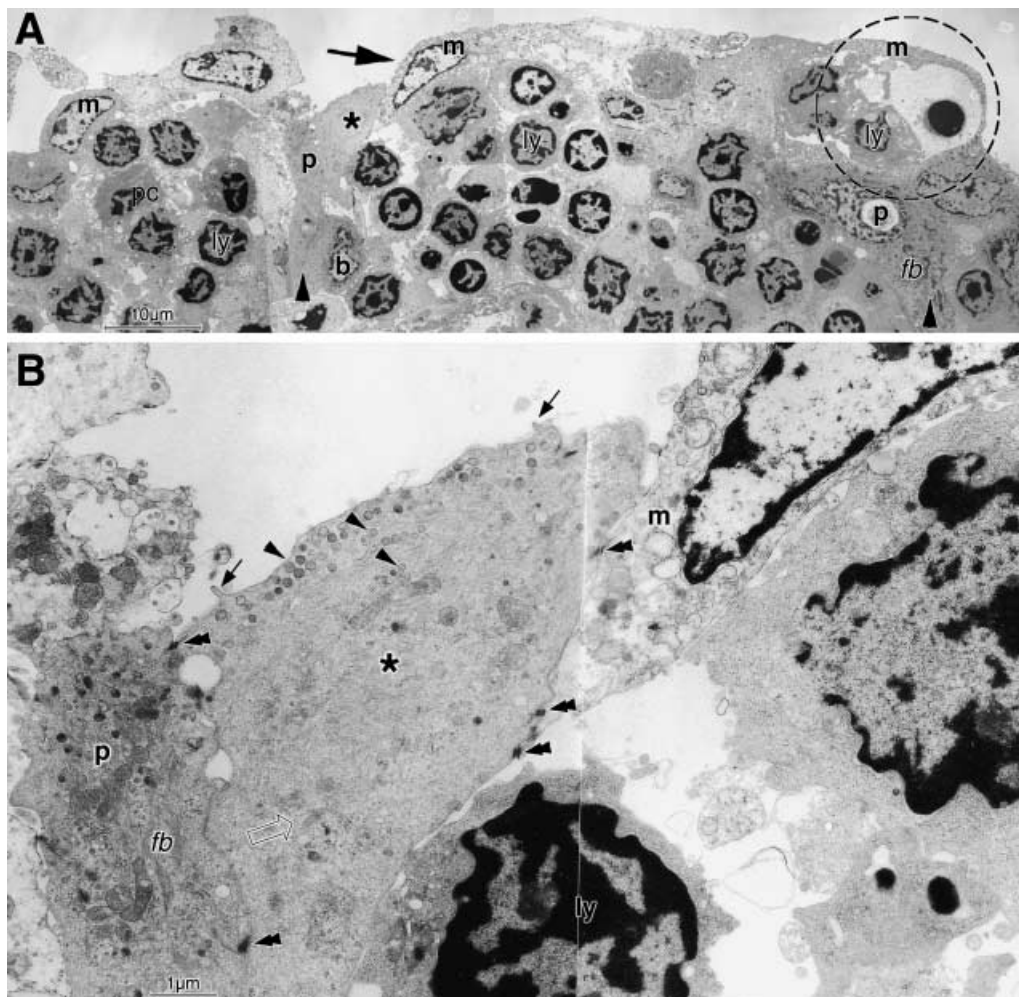
Fig. 8 In TEM overview, the FAE is seen to be densely populated by lymphoid cells (ly) arranged in groups; a plasma cell (pc) also occurs. They are separated by electron-dense epithelial cells forming basal cells (b) and pillars (p and large arrowhead, compare with Fig. 2B) that reach up between the lymphocytes. They are covered by superficial electron-lucent M-cells with a large pale nucleus (m and large arrow). The configuration at the right side (interrupted circle) resembles that seen in SEM (Fig. 7G). At higher magnification the dark pillar cell (p) is shown to contain dense bundles of intermediate filaments (fb) which are absent from the M-cell. An intermediate cell type with medium electron density (asterisk in A,B) is interposed between dense and lucent cells. It has a darker cytoplasm than M-cells but contains only one small, faint intermediate filament bundle (open arrow in B) and the cytoplasm is filled with a diffuse meshwork of filaments. Small vesicles (arrowheads) occur beneath the outer cell membrane and inside the cell; some short microvilli are present at the surface (arrows in B). All three cell types are connected by desmosomes (double arrowheads in B). Scale bars = 10 μm in A, 1 μm in B.

surface, accumulate in the lacrimal lake before they disappear into the lacrimal drainage system. This is further supported by the continuation of MALT inside the rabbit lacrimal drainage system (Knop & Knop, 1996).

The previous description of the epithelium overlying rabbit CALT follicles as a lympho-epithelium was based on light microscopical findings together with a preliminary SEM description of cells with different content of surface microprojections (Chandler & Axelrod, 1980) and suggested a similarity with the gut- and bronchus-associated lymphoid tissues. In addition, we have characterized this epithelium as a regular FAE, by investigating the ultrastructural anatomy of the follicles in TEM and in stereoscopic SEM. With these techniques it was possible to identify antigen-transporting M-cells in the FAE based on the presence of several ultrastructural characteristics that appear in sharp contrast to adjacent non-M-cells. In the multilayered rabbit CALT they form an intraepithelial cavernous network and have a structural arrangement that is slightly different from GALT and BALT.
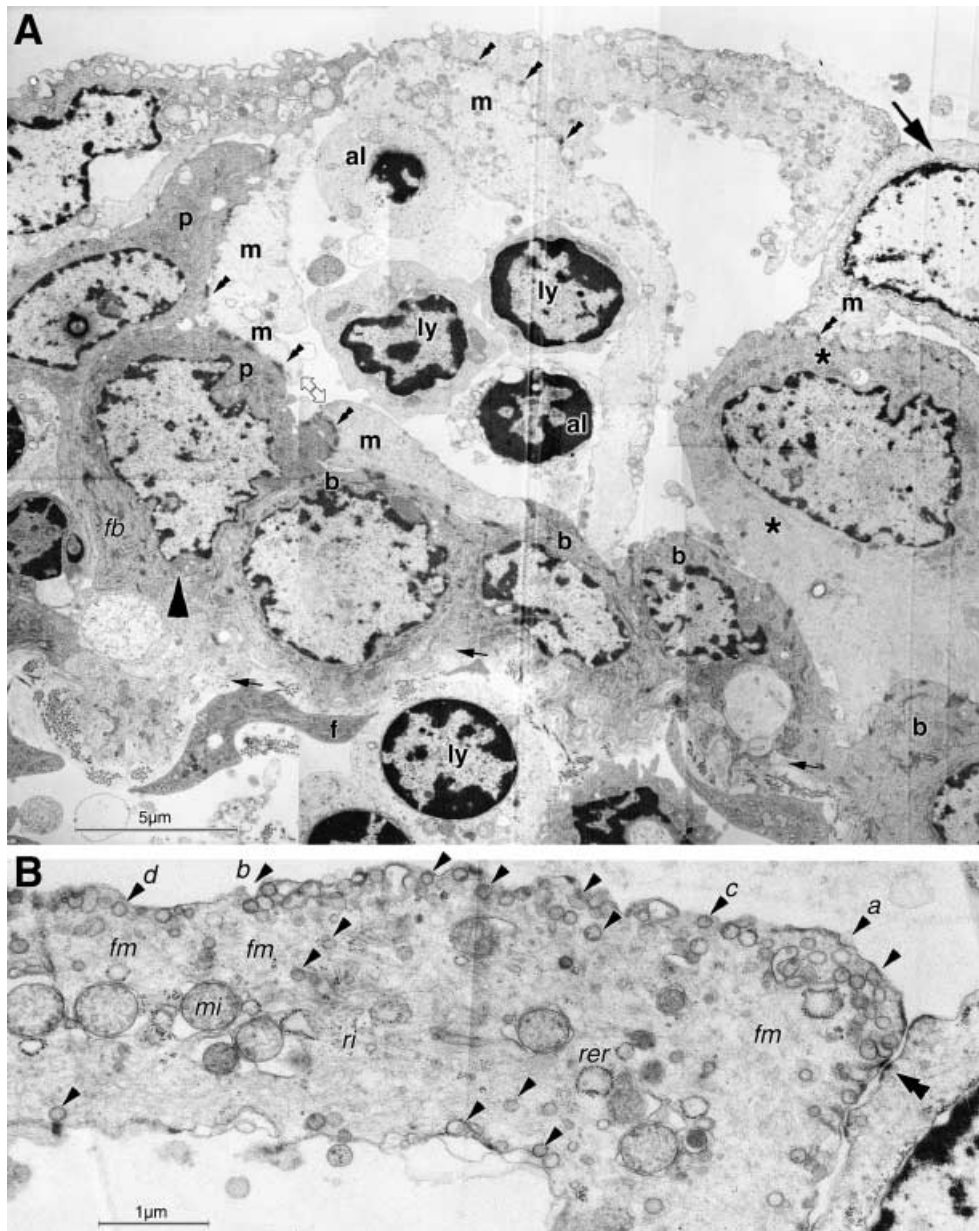
Fig. 9 Epithelial basal and pillar cells (p and large arrowhead in A; compare with Fig. 2B) form a cavity that has a roof formed by two bright M-cells (m and large arrow). The left one forms a thin wallpaper-like lining along the darker cells and a septation in the middle of the epithelial cavity. It hence wraps the lymphocytes (ly) in a cytoplasmic pocket; two lymphoid cells in the pocket appear apoptotic. Another M-cell assists to cover the luminal surface at the right side and an intermediate cell type is present beneath (asterisks). A small opening is seen in the M-cell cytoplasm at the left lateral side (double open arrow) and a basal area, and the intermediate cell to the right is uncovered. All epithelial cells are connected by desmosomes (double arrowheads). Small arrows indicate the level of the epithelial basement membrane. In the lamina propria are fibrocytes (f) and lymphocytes; one (ly) is directly under the basement membrane and appears to cause it to bulge outward, probably in transit to the M-cell pocket. At higher magnification (B), the luminal cytoplasmic lamina of an M-cell is seen to contain, in addition to mitochondria (mi), ribosomes (ri) and occasional rough endoplasmic reticulum (rer), a fine filament meshwork (fm) and numerous endocytotic vesicles (arrowheads). The luminal surface shows different stages of endocytosis (a–d). Scale bars = 5 µm in A; 1 µm in B.

The present paper also shows that the previously undescribed ultrastructure of specialized HEV in the parafollicular zone of rabbit CALT follicles has a characteristic morphology similar to human CALT (Knop & Knop, 1998a,b) and to other lymphoid organs (Anderson & Anderson, 1976). HEV are an important requisite for the regulated immigration of lymphoid cells from the blood into MALT (Kraal & Mebius, 1997) and also into
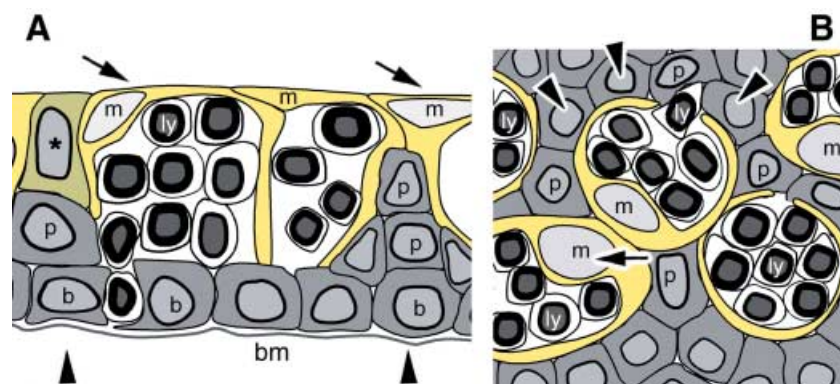
Fig. 10 The presumed structure of the follicle-associated epithelium (FAE) in the rabbit CALT is schematically indicated in cross (A) and tangential (B) section through at about mid-height, according to our observations; compare with Fig. 2(B,C). The ordinary darker epithelial cells form basal cells (b) resting on the basement membrane (bm) and pile up or elongate into pillars (p and arrowhead). Together they build a cavity. The delicately constructed brighter M-cells with a pale nucleus (m and arrow) form a thin wallpaper-like cytoplasmic lamella and rest between and on top of the darker cells, which can serve as a mechanical support and scaffold to hold the M-cells in place at the luminal surface. More than one M-cell can form a roof over a cavity and they can form septations; their luminal lamellae overlap over a certain distance. The cytoplasmic pockets of the M-cells contain lymphoid cells (ly) and have natural basal openings for their migration. A cell with intermediate density (asterisk) is interposed between dark and bright cells.

CALT as seen here. The migration is regulated by adhesion molecules, which also occur on ocular-surface HEV (Haynes et al. 1999), and these molecules are produced and externalized by the endothelial cells. Evidence for this process is indicated in the present study by the observation of a prominent apical Golgi apparatus in the endothelial cells and of secretory vesicles that originate from it and fuse with the apical cell membrane, in particular where this is in contact with an intraluminal lymphocyte. Endothelial lamellopodia in the contact area further support an active cross-talk of the HEV in rabbit CALT with lymphoid cells. It is interesting to note that a transformation of HEV into ordinary post-capillary venules can be directly observed in vessels that leave the parafollicular zone and are viewed in tangential section. This indicates that HEV are a special morphological and functional adaptation of post-capillary venules to the requirements of efficient, regulated lymphocyte migration in lymphoid tissues. Together with the known lymphatic vessels for the eventual return of lymphocytes via lymph nodes and the thoracic duct into the blood circulation, HEV connect the ocular lymphoid tissue to the other organs of the mucosal immune system and hence further characterize the ocular surface as a part of the MALT system (Knop & Knop, 2004b).

Inside the FAE covering the apex of the rabbit CALT follicles, cells with several typical ultrastructural characteristics of M-cells were identified, which differ in their shape and in the composition of the cytoplasm from ordinary epithelial cells. They form large cytoplasmic pockets containing groups of lymphoid cells and separate them from the lumen only by a narrow membranous cytoplasmic layer. Their cytoplasm is more light- and electron-lucent than the surrounding epithelial cells, as reported for M-cells in general (Gebert, 1997). They have signs of cell activity as bright euchromatic nuclei, as also observed, for example, in M-cells of the human intestine (Farstad et al. 1994) with a prominent nucleolus indicating active mRNA transcription. They show numerous endocytotic vesicles for the uptake and transcytotic transport of luminal antigens towards the lymphoid cells in the pocket, which is considered to represent the main function of M-cells (Gebert & Bartels, 1995; Neutra et al. 1996b). The ultrastructural evidence for an endocytotic apparatus in the present study is supported by recent findings of a selective uptake of substances over rabbit CALT follicles (Liu et al. 2004; Astley & Chodosh, 2005). Luminal antigens are then transported by the lymphoid cells, or by dendritic cells from the M-cell pockets to the follicular zones for antigen presentation (Farstad et al. 1994) and for the initiation of immune reactions.

These events can result in the formation of a bright germinal centre (Wolniak et al. 2004) of proliferating lymphocytes as was indeed found here in the rabbit CALT follicles. We found evidence for proliferating lymphoblasts and for FDC that continuously provide antigens on their surface related to the presence of prominent vesicles in their cytoplasm, as observed here and in other lymphoid tissues (Szakal et al. 1983),

and considered to support the differentiation of the proliferating lymphoblasts (Wolniak et al. 2004). There was also evidence for apoptotic lymphocytes in rabbit CALT GC, which are a typical characteristic of GC because differentiating lymphocytes are induced to die when they exhibit inappropriate antigen specificity or binding affinity. The observed tingible body macrophages serve for cell debris uptake and destruction. In contrast to an earlier investigation that did not observe plasma cells in rabbit CALT follicles by immunohistochemistry (Franklin & Remus, 1984), we observed them occasionally in the FAE by TEM.

Other criteria further support our diagnosis of M-cells, such as the diffuse meshwork of fine filaments, because M-cells generally have a less elaborate intermediate filament system and similar filaments have been described in M-cells of other mucosal organs (Gebert, 1997). These filaments may correspond to vimentin immunoreactivity inside the FAE of rabbit CALT (Liu et al. 2004), BALT (Gebert & Hach, 1992) and tonsils (Gebert et al. 1995), which is regarded as a general rabbit M-cell marker. Cells with a different content or shape of microprojections at the luminal surface (smooth compared with microvilli) also support the diagnosis of interspersed M-cells (Chandler & Axelrod, 1980). However, although the surface of M-cells usually seems to differ from that of surrounding cells, their exact morphology (i.e. short or long, frequent or few microprojections) varies in different organs and even in different zones of the same organ (intestine) (Jepson et al. 1993; Gebert et al. 1996), and is therefore not sufficient to verify that they are M-cells.

The structural arrangement of M-cells in the FAE, as seen in the present study, appears to be a special and undescribed characteristic of CALT. In the FAE of 'conventional' organs of the mucosal immune system such as the intestine, the epithelium is simple (mono-layered) and M-cells are resting directly on the basement membrane because they are able to span the whole epithelial height. By contrast, the conjunctival epithelium is stratified (multilayered). This may explain why M-cells only occur in the superficial layer of the CALT FAE and rest here on top of and between ordinary basal and 'pillar' epithelial cells, which span a part of the epithelial height and also appear necessary to provide a scaffold that stabilizes the delicate meshwork of the fragile thin-walled 'lymphocyte containers'. Together with the observed pillars or fences, as depicted in the schematic drawings of Fig. 10, that are built by the basal epithelial cells, this construction appears to represent a special

structural requirement for the multilayered morphology of the conjunctival epithelium. The luminal cells with a delicate superficial cytoplasmic lamina that covers large cavernous spaces filled by lymphoid cells and conceivably ruptures easily during the preparation are similar to M-cells in the FAE of palatine tonsils that also reside in a multilayered epithelium (Howie, 1980).

The observation of cells with medium electron density, interposed between the ordinary electron-dense epithelial cells and the electron-lucent M-cells, suggests that they could represent intermediate stages during the development of M-cells from local epithelial cells. Contradictory evidence for the development of M-cells is provided in the literature (Kraehenbuhl & Neutra, 2000). Some studies have assumed that M-cells originate from the crypts in mouse Peyer's patch (Bye et al. 1984) and rabbit caecum (Jepson et al. 1993) because immature precursors were observed in the follicle periphery. In rabbit caecal patch they even appear to have a different clonal origin from different crypts (Gebert & Posselt, 1997). Another line of evidence, however, seems to indicate that M-cells develop locally in the FAE by conversion of epithelial cells under the influence of immune cells, for example in the sheep palatine tonsil (Olah et al. 1988), in mouse Peyer's patch (Smith & Peacock, 1992) or in the gut in general (Hamzaoui & Pringault, 1998). This is regulated by different factors as found in knockout mice (Debard et al. 1999), including the influence of stromal cells (Kraehenbuhl & Neutra, 2000). Different co-culture models of enterocytes with lymphoid cells resulted in the development of cells with characteristics of M-cells (Gullberg et al. 2000; van der Lubben et al. 2002) and have proven this basic concept.

It thus appears likely that the cells with intermediate morphology that were observed in the present study indeed represent epithelial cells that move upward in the epithelium and transform into the M-cell phenotype. Small holes observed occasionally where several M-cells meet may represent natural openings (in contrast to the artificially fractured cells) and could either indicate that lymphoid cells are physiologically released onto the ocular surface or that M-cells at the end to their life cycle are about to be shed. An indication for apparently naturally shed cells was observed here by using SEM (Fig. 7G,H). In this case, the intermediate cells would be necessary and in an appropriate position, as seen in Fig. 9(A), to replace them.

Earlier findings of M-cells in CALT of different species were not unequivocally accepted (Chodosh et al. 1998a)

and these cells were not observed in a number of species (Chodosh et al. 1998b), although several studies have since reported morphological and increasing functional evidence for M-cells. They were first reported in the guinea-pig (Latkovic, 1989), and a selective substance uptake by them was controversial and not found for horseradish peroxidase (Stock et al. 1987) but was reported for peroxidase–antiperoxidase (Shoji et al. 1998). Although in an early electron microscopic study of rabbit CALT, distinctive M-cells were not reported (Gebert & Bartels, 1990), ultrastructural characteristics of M-cells were later found (Knop & Knop, 1998c,d). Light microscopical indication for M-cells was observed in the human conjunctiva (Knop & Knop, 1998d, 2000) and lacrimal drainage system (Knop & Knop, 2001). M-cells were identified ultrastructurally in CALT of the cynomolgus monkey (Ruskell, 1995; Ruskell & VanderWerf, 1997) and in the nictitating membrane of the dog (Giuliano et al. 2002).

Functional evidence for a selective uptake of substances in the FAE was found in the dog (Giuliano et al. 2002), guinea-pig (Shoji et al. 1998) and recently rabbit (Liu et al. 2004; Astley & Chodosh, 2005). Evidence for an afferent immune function of CALT, e.g. in the induction of tolerance, was observed after topical conjunctival instillation of antigen. This is able to prevent intraocular inflammation in the rat (Dua et al. 1994) or can be used as immunotherapy in order to abolish symptoms in animal models of ocular allergy (Bielory & Mongia, 2002) and in human patients (Nunez & Cuesta, 2000). This may indicate that the generation of physiological immunological tolerance is a main function of CALT, as of MALT in general (McGhee et al. 1999). The functionality of rabbit CALT follicles for active ocular immune protection is indicated by the fact that their B-cells can differentiate into IgA-positive plasma cell precursors after antigen stimulation (Franklin & Remus, 1984). This is supported in the present study by the finding of lymphoblasts in the GC that require previous uptake of antigen.

In conclusion, the presence of CALT in the rabbit with follicular M-cells, GC and para-follicular HEV further supports the concept of an EALT (Knop & Knop, 2001, 2002, 2005) at the ocular surface and supports the general integration of the ocular mucosal tissues into the mucosal immune system of the body.

Acknowledgements

References

Anderson AO, Anderson ND (1976) Lymphocyte emigration from high endothelial venules in rat lymph nodes. *Immunology* **31**, 731–748.

Astley RA, Chodosh J (2005) Selective uptake of iron oxide by rabbit conjunctival lymphoid follicles. *Cornea* **24**, 334–336.

Aurell G (1938) Kolophonium-Chininhydrochloridgemische als Einschlussmittel für sehr dicke Schnitte zu mikroskopischen Zwecken. *Z. Wiss Mikr* **55**, 256–273.

Axelrod AJ, Chandler JW (1979) Morphologic characteristics of conjunctival lymphoid tissue in the rabbit. In *Proceedings of the Second International Symposium on the Immunology and Immunopathology of the Eye* (eds Silverstein AM, Connor GR), pp. 292–301. New York: Masson Publishing.

Bielory L, Mongia A (2002) Current opinion of immunotherapy for ocular allergy. *Curr Opin Allergy Clin Immunol* **2**, 447–452.

Bienenstock J, McDermott M, Befus D, O'Neill M (1978) A common mucosal immunologic system involving the bronchus, breast and bowel. *Adv Exp Med Biol* **107**, 53–59.

Brandtzaeg P (1996) History of oral tolerance and mucosal immunity. *Ann NY Acad Sci* **778**, 1–27.

Butcher EC, Picker LJ (1996) Lymphocyte homing and homeostasis. *Science* **272**, 60–66.

Bye WA, Allan CH, Trier JS (1984) Structure, distribution, and origin of M cells in Peyer's patches of mouse ileum. *Gastroenterology* **86**, 789–801.

Chandler JW, Axelrod AJ (1980) Conjunctiva-associated lymphoid tissue: a probable component of the mucosa-associated lymphoid system. In *Immunologic Diseases of the Mucous Membrane: Pathology, Diagnosis and Treatment* (ed. Connor GR), pp. 63–70. New York: Masson Publishing.

Chodosh J, Nordquist RE, Kennedy RC (1998a) Anatomy of mammalian conjunctival lymphoepithelium. *Adv Exp Med Biol* **438**, 557–565.

Chodosh J, Nordquist RE, Kennedy RC (1998b) Comparative anatomy of mammalian conjunctival lymphoid tissue: a putative mucosal immune site. *Dev Comp Immunol* **22**, 621–630.

Chodosh J, Kennedy RC (2002) The conjunctival lymphoid follicle in mucosal immunology. *DNA Cell Biol* **21**, 421–433.

Dana MR, Qian Y, Hamrah P (2000) Twenty-five-year panorama of corneal immunology: emerging concepts in the immunopathogenesis of microbial keratitis, peripheral ulcerative keratitis, and corneal transplant rejection. *Cornea* **19**, 625–643.

Debard N, Sierro F, Kraehenbuhl JP (1999) Development of Peyer's patches, follicle-associated epithelium and M cell: lessons from immunodeficient and knockout mice. *Semin Immunol* **11**, 183–191.

Dua HS, Donoso LA, Laibson PR (1994) Conjunctival instillation of retinal antigens induces tolerance. *Ocular Immunol Inflammation* **2**, 29–36.

Farstad IN, Halstensen TS, Fausa O, Brandtzaeg P (1994) Heterogeneity of M-cell-associated B and T cells in human Peyer's patches. *Immunology* **83**, 457–464.

Franklin RM, Remus LE (1984) Conjunctival-associated lymphoid tissue: evidence for a role in the secretory immune system. *Invest Ophthalmol Vis Sci* **25**, 181–187.

Gebert A, Bartels H (1990) Ultrastruktur des follikel-assoziierten Epithels in der Konjunktiva des Kaninchens. *Verh Anat Ges (Anat Anz Suppl)* **166**, 359–360.

Gebert A, Hach G (1992) Vimentin antibodies stain membranous epithelial cells in the rabbit bronchus-associated lymphoid tissue (BALT). *Histochemistry* **98**, 271–273.

Gebert A, Bartels H (1995) Ultrastructure and protein transport of M cells in the rabbit cecal patch. *Anat Rec* **241**, 487–495.

Gebert A, Willfuhr B, Pabst R (1995) The rabbit M-cell marker vimentin is present in epithelial cells of the tonsil crypt. *Acta Otolaryngol Stockh* **115**, 697–700.

Gebert A, Rothkotter HJ, Pabst R (1996) M cells in Peyer's patches of the intestine. *Int Rev Cytol* **167**, 91–159.

Gebert A (1997) The role of M cells in the protection of mucosal membranes. *Histochem Cell Biol* **108**, 455–470.

Gebert A, Posselt W (1997) Glycoconjugate expression defines the origin and differentiation pathway of intestinal M-cells. *J Histochem Cytochem* **45**, 1341–1350.

Giuliano EA, Moore CP, Phillips TE (2002) Morphological evidence of M cells in healthy canine conjunctiva-associated lymphoid tissue. *Graefes Arch Clin Exp Ophthalmol* **240**, 220–226.

Gowans JL, Knight EJ (1964) The route of re-circulation of lymphocytes in the rat. *Proc Soc Exp Biol Med* **159**, 257–282.

Gullberg E, Leonard M, Karlsson J, et al. (2000) Expression of specific markers and particle transport in a new human intestinal M-cell model. *Biochem Biophys Res Commun* **279**, 808–813.

Hamzaoui N, Pringault E (1998) Interaction of microorganisms, epithelium, and lymphoid cells of the mucosa-associated lymphoid tissue. *Ann NY Acad Sci* **859**, 65–74.

Haynes RJ, Tighe PJ, Scott RA, Dua HS (1999) Human conjunctiva contains high endothelial venules that express lymphocyte homing receptors. *Exp Eye Res* **69**, 397–403.

Howie AJ (1980) Scanning and transmission electron microscopy on the epithelium of human palatine tonsils. *J Pathol* **130**, 91–98.

Jepson MA, Clark MA, Simmons NL, Hirst BH (1993) Epithelial M cells in the rabbit caecal lymphoid patch display distinctive surface characteristics. *Histochemistry* **100**, 441–447.

Jepson MA, Clark MA, Hirst BH (2004) M cell targeting by lectins: a strategy for mucosal vaccination and drug delivery. *Advanced Drug Delivery Rev* **56**, 511–525.

Karnovsky MJ (1965) A formaldehyde–glutaraldehyde fixative of high osmolarity for use in electron microscopy. *J Cell Biol* **27**, 137–138.

Kessing SV (1968) Mucous gland system of the conjunctiva. A quantitative normal anatomical study. *Acta Ophthalmol Copenh Suppl* **95**, 1–133.

Knop E, Knop N (1996) MALT tissue of the conjunctiva and nasolacrimal system in the rabbit and human. *Vision Res* **36**, S60.

Knop E, Knop N (1998a) Fine structure of high endothelial venules in the human conjunctiva. *Ophthalmic Res* **30**, 169.

Knop E, Knop N (1998b) High endothelial venules are a normal component of lymphoid tissue in the human conjunctiva and lacrimal sac. *Invest Ophthalmol Vis Sci* **39**, S548.

Knop N, Knop E (1998c) Cells with m-cell characteristics in the follicle associated epithelium of the rabbit conjunctiva. *Ophthalmic Res* **30** (Suppl. 1, 392), 82.

Knop N, Knop E (1998d) M-cells of the conjunctiva associated lymphoid tissue (CALT) in the rabbit and human. *Invest Ophthalmol Vis Sci* **39**, 548.

Knop N, Knop E (2000) Conjunctiva-associated lymphoid tissue in the human eye. *Invest Ophthalmol Vis Sci* **41**, 1270–1279.

Knop E, Knop N (2001) Lacrimal drainage associated lymphoid tissue (LDALT): A part of the human mucosal immune system. *Invest Ophthalmol Vis Sci* **42**, 566–574.

Knop E, Knop N (2002) A functional unit for ocular surface immune defense formed by the lacrimal gland, conjunctiva and lacrimal drainage system. *Adv Exp Med Biol* **506**, 835–844.

Knop E, Knop N (2003) Augen-assoziiertes lymphatisches Gewebe (EALT) durchzieht die Augenoberfläche kontinuierlich von der Tränendrüse bis in die ableitenden Tränenwege. *Ophthalmologe* **100**, 929–942.

Knop E, Knop N, Brewitt H (2003) [Dry eye disease as a complex dysregulation of the functional anatomy of the ocular surface. New impulses to understanding dry eye disease]. *Ophthalmologe* **100**, 917–928.

Knop E, Knop N (2004a) Eye associated lymphoid tissue (EALT) and the ocular surface. In *Proceedings of the 5th International Symposium on Ocular Pharmacology and Therapy*, pp. 91–98. Bologna: Medimond.

Knop E, Knop N (2004b) Lymphocyte homing in the mucosal immune system to the eye-associated lymphoid tissue (EALT). In *Immunology of the Ocular Surface and Tearfilm* (eds Zierhut M, Sullivan DA, Stern ME), pp. 35–72. Amsterdam: Swets and Zeitlinger.

Knop E, Knop N, Pleyer U (2004) Clinical aspects of MALT. In *Uveitis and Immunological Disorders* (eds Pleyer U, Mondino B), pp. 67–89. Berlin: Springer Verlag.

Knop E, Knop N (2005) The role of eye-associated lymphoid tissue in corneal immune protection. *J Anat* **206**, 271–285.

Kraal G, Mebius RE (1997) High endothelial venules: lymphocyte traffic control and controlled traffic. *Adv Immunol* **65**, 347–395.

Kraehenbuhl JP, Neutra MR (2000) Epithelial M cells: differentiation and function. *Annu Rev Cell Dev Biol* **16**, 301–332.

Latkovic S (1989) Ultrastructure of M cells in the conjunctival epithelium of the guinea pig. *Curr Eye Res* **8**, 751–755.

Liu H, Meagher CK, Moore CP, Phillips TE (2004) Antigen sampling M cells in the rabbit conjunctiva. *Invest Ophthalmol Visual Sci* **45**, 1505.

van der Lubben I, van Opdorp FA, Hengeveld MR, et al. (2002) Transport of chitosan microparticles for mucosal vaccine delivery in a human intestinal M-cell model. *J Drug Target* **10**, 449–456.

McGhee JR, Lamm ME, Strober W (1999) Mucosal immune responses. An overview. In *Handbook of Mucosal Immunology* (eds Ogra PL, Mestecky J, Lamm ME, Strober W, McGhee JR, Bienenstock J), pp. 485–506. San Diego: Academic Press.

Mestecky J, McGhee JR, Michalek SM, Arnold RR, Crago SS, Babb JL (1978) Concept of the local and common mucosal immune response. *Adv Exp Med Biol* **107**, 185–192.

Neutra MR, Frey A, Kraehenbuhl JP (1996a) Epithelial M cells: gateways for mucosal infection and immunization. *Cell* **86**, 345–348.

Neutra MR, Pringault E, Kraehenbuhl JP (1996b) Antigen sampling across epithelial barriers and induction of mucosal immune responses. *Annu Rev Immunol* **14**, 275–300.

Niimi Y (1935) Studien über den Lymphfollikel in der Conjunctiva. I. Mitt. Über den Lymphfollikel in der Conjunctiva bei normalen Kaninchen. *Acta Soc Ophthal Japan* **39**, 808–823.

Nunez JA, Cuesta U (2000) Local conjunctival immunotherapy: the effect of dermatophagoides pteronyssinus local conjunctival immunotherapy on conjunctival provocation test in patients with allergic conjunctivitis. *Allergol Immunopathol (Madr)* **28**, 301–306.

Olah I, Takacs L, Toro I (1988) Formation of lymphoepithelial tissue in the sheep's palatine tonsil. *Acta Otolaryngol Suppl* **454**, 7–17.

Owen RL, Jones AL (1974) Epithelial cell specialization within human Peyer's patches: an ultrastructural study of intestinal lymphoid follicles. *Gastroenterology* **66**, 189–203.

Pabst R, Westermann J (1997) Lymphocyte traffic to lymphoid and non-lymphoid organs in different species is regulated by several mechanisms. In *Adhesion Molecules and Chemokines in Lymphocyte Trafficking* (ed. Hamann, A), pp. 21–37. Amsterdam: Harwood Academic Publishers.

Paulsen FP, Paulsen JI, Thale AB, Schaudig U, Tillmann BN (2002) Organized mucosa-associated lymphoid tissue in human naso-lacrimal ducts. *Adv Exp Med Biol* **506**, 873–876.

Pflugfelder SC, Solomon A, Stern ME (2000) The diagnosis and management of dry eye: a twenty-five-year review. *Cornea* **19**, 644–649.

Ruskell GL (1995) Organization and cytology of lymphoid tissue in the cynomolgus monkey conjunctiva. *Anat Rec* **243**, 153–164.

Ruskell GL, VanderWerf F (1997) Sensory innervation of conjunctival lymph follicles in cynomolgus monkeys. *Invest Ophthalmol Vis Sci* **38**, 884–892.

Shoji J, Inada N, Saito K, Takaura N, Iwasaki Y, Sawa M (1998) Immunohistochemical study on follicular dendritic cell of conjunctiva-associated lymphoid tissue. *Jpn J Ophthalmol* **42**, 1–7.

Smith ME, Finke EH (1972) Critical point drying of soft biological material for the scanning electron microscope. *Invest Ophthalmol Visual Sci* **11**, 127–132.

Smith MW, Peacock MA (1992) Microvillus growth and M-cell formation in mouse Peyer's patch follicle-associated epithelial tissue. *Exp Physiol* **77**, 389–392.

Stern ME, Gao J, Schwalb TA, et al. (2002) Conjunctival T-cell subpopulations in Sjogren's and non-Sjogren's patients with dry eye. *Invest Ophthalmol Vis Sci* **43**, 2609–2614.

Stock EL, Sobut RA, Roth SI (1987) The uptake of horseradish peroxidase by the conjunctival epithelium of the guinea-pig. *Exp Eye Res* **45**, 327–337.

Szakal AK, Holmes KL, Tew JG (1983) Transport of immune complexes from the subcapsular sinus to lymph node follicles on the surface of nonphagocytic cells, including cells with dendritic morphology. *J Immunol* **131**, 1714–1727.

Virchow H (1910) Mikroskopische Anatomie der äusseren Augenhaut und des Lidapparates. In *Graefe-Saemisch Handbuch der Gesamten Augenheilkunde, Band 1, 1 Abteilung, Kapitel II* (ed. Saemisch T), p. 431. Leibzig: Verlag W. Engelmann.

Wolf JL, Rubin DH, Finberg R, et al. (1981) Intestinal M cells: a pathway for entry of reovirus into the host. *Science* **212**, 471–472.

Wolniak KL, Shinall SM, Waldschmidt TJ (2004) The germinal center response. *Crit Rev Immunol* **24**, 39–65.